Liquid Crystals
Publication details, including instructions for authors and subscription information:
http://www.informaworld.com/smpp/title~content=t713926090

Synthesis and mesomorphic properties of semi-fluorinated chiral liquid crystals with a tribenzoate mesogenic core

Shune-Long Wu[a]; Cho-Ying Lin[a]
[a] Department of Chemical Engineering, Tatung University, Taipei, Taiwan 104 ROC

To cite this Article Wu, Shune-Long and Lin, Cho-Ying(2007) 'Synthesis and mesomorphic properties of semi-fluorinated chiral liquid crystals with a tribenzoate mesogenic core', Liquid Crystals, 34: 1, 25 — 31
To link to this Article: DOI: 10.1080/02678290601076494
URL: http://dx.doi.org/10.1080/02678290601076494

Liquid Crystals, Vol. 34, No. 1, January 2007, 25–31

Synthesis and mesomorphic properties of semi-fluorinated chiral liquid crystals with a tribenzoate mesogenic core

SHUNE-LONG WU* and CHO-YING LIN

Department of Chemical Engineering, Tatung University, 40, Chungshan N. Rd., 3rd Sec., Taipei, Taiwan 104 ROC

(*Received 30 June; accepted 28 July 2006*)

A novel series of semi-fluorinated chiral liquid crystals, derived from a tribenzoate mesogenic core and a (*S*)-1-methyl-2-(2,2,3,3,3-pentafluoropropyloxy)ethyl chiral tail, was prepared and the mesomorphic phases investigated. It was found that materials with shorter alkyl chain length (m=8 to 10) favour the formation of an antiferroelectric SmC^*_A phase, and those with longer chain length (m=9 to 12) favour the formation of a ferroelectric SmC* phase. One SmC^*_α subphase was found at material m=9. The basic electro-optical properties of the chiral materials in SmC* and SmC^*_A phases were measured. The results show that the maximum $\mathbf{P}_s$ values are in the range 66–72 nC cm^{-2} and the maximum apparent tilt angles are in the range 29°–34°.

1. Introduction

Since the discovery of antiferroelectricity in the liquid crystal materials (*R*)- or (*S*)-4-(1-methylheptyloxycarbonyl) phenyl 4′-octyloxybiphenyl-4-carboxylate (MHBOPC), in 1988 by Chandani *et al.* [1], the SmC^*_A phase has been paid much attention. Up to now, most antiferroelectric liquid crystal materials have a molecular design similar to that of MHBOPC, having a bipenyl-phenyl core structure to exhibit the SmC^*_A phase [1–6]. Extended studies on some materials having a tribenzoate mesogenic core [7–12] indicate that not only does it yield a stronger and broader range of the ferroelectric SmC* phase and a less frequent appearance of the antiferroelectric SmC^*_A phase, but it also leads to other polymorphism, with subphases such as SmC^*_α, SmC^*_{FI1} and SmC^*_{FI2}. Therefore, because the structure and physical properties of these subphases are not yet clear, this has become an interesting field of research, and many studies of the molecular arrangement and physical properties of these phases have been made [13–19].

Our previous study on a series of semi-fluorinated chiral materials MPFPECP*m*BC(m=8–12), which have a biphenyl-phenyl core structure and a semi-fluorianted (*S*)-1-methyl-2-(2,2,3,3,3-pentafluoropropyloxy)ethyl chiral tail, shows that all the materials possess an antiferroelectric SmC^*_A phase with rather wide temperature ranges [20, 21]. In order to obtain a greater impact of this semi-fluorinated chiral moiety on the mesophases and physical properties of to these mesophases, we have designed and synthesized a homologous series of tribenzoate materials, the (*R*)-4-[1-methyl-2-(2,2,3,3,3-pentafluoropropyloxy)ethyl 4-{4-[4-(alkyloxybenzoyloxy)benzoyloxy]}benzoates, MPFPE*m*BBB (m=8–12) (formula 1), for investigation. The general structural formula for this series of materials is depicted below.

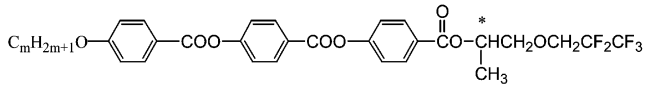

MPFPE*m*BBB(m=8-12)

2. Experimental

2.1. *Characterization of the materials*

The chemical structures for the intermediates and target materials were analysed by nuclear magnetic resonance spectroscopy using a JEOL EX-400 FT-NMR spectrometer. Infrared spectra were recorded on a Horiba FT-720 Fourier transform infrared (FTIR) spectrometer. The purity was determined by thin layer chromatography and further confirmed by elemental analysis using a Perkin-Elmer 2400 spectrometer. Transition temperatures and phase transition enthalpies of the materials were determined by differential scanning calorimetry using a Perkin-Elmer DSC7 calorimeter at running rates of 5°C min^{-1}. Mesophases were principally identified from the microscopic texture of the materials sandwiched between two glass plates under a crossed

*Corresponding author. Email: slwu@ttu.edu.tw

Liquid Crystals
ISSN 0267-8292 print/ISSN 1366-5855 online © 2007 Taylor & Francis
http://www.tandf.co.uk/journals
DOI: 10.1080/02678290601076494

polarizing microscope using a Nikon Microphot-FXA in conjunction with a Mettler FP82 hot stage.

The physical properties of the ferroelectric and antiferroelectric phases of the materials were measured in 5 μm homogeneously aligned cells, which were purchased from E. H. C. Co. Japan. The spontaneous polarization ($\mathbf{P}_s$) was measured by a triangular wave method [22]. The measurement of optical transmittance versus applied electric field was conducted by using a He-Ne laser (5 mW, 632.8 nm) as a probe beam [1, 23]. The optical transmittance of the probe beam passing though the cell between crossed polarizers, whose axes were parallel and perpendicular to the smectic layer normal, was detected by a photodiode. The signals were detected with a HP54502A digital oscilloscope. The voltage applied to the electric field was produced by an arbitrary wave-form generator (AG1200) and amplified by a home-made power preamplifier.

2.2. *Preparation of materials*

The starting chiral materials, (*S*)-propylene oxide and 2,2,3,3,3-pentafluoro-1-propanol, were purchased from Aldrich Co. Chem., with purity greater than 99%. Thin layer chromatography was performed with TLC sheets coated with silica; spots were detected by UV irradiation. Silica gel (MN kieselgel 60, 70–230 mesh) was used for column chromatography. Anhydrous organic solvents, dichloromethane (CH_2Cl_2) and tetrahydrofuran (THF), were purified by treatment with CaH_2 and $LiAlH_4$, respectively, and distilled before use.

The synthetic processes for the target materials MPFPE*m*BBB(*m*=8–12) were carried out as outlined in scheme 1. The detailed procedures for the syntheses of the materials are described as follows.

2.2.1. (*R*)-1-methyl-2-(2,2,3,3,3-pentafluoropropyloxy) ethyl 4-(methoxycarbonyloxy)benzoate. This compound was prepared following a method reported in literature [21].

2.2.2. (*R*)-1-Methyl-2-(2,2,3,3,3-pentafluoropropyloxy) ethyl 4-hydroxybenzoate, 1. This compound was also prepared as reported in [21].

2.2.3. (*R*)-1-Methyl-2-(2,2,3,3,3-pentafluoropropyloxy) ethyl 4-[4-(methoxycarbonyloxy)benzoyloxy]benzoate, 2. Oxalyl chloride ($(COCl)_2$; 2.85 ml, 32.5 mmol) was added slowly to 4-methoxycarbonyloxybenzoic acid (2.55 g, 13 mmol) in dichloromethane (50 ml) and the resulting solution was heated under reflux with stirring for 2 h. Excess oxalyl chloride was removed by evaporation under reduced pressure. The crude 4-methoxycarbonyloxybenzoic acid chloride in dichloromethane (5 ml) was added to a solution of compound 1 (3.28 g, 10 mmol) and triethylamine (TEA; 5 ml) in dichloromethane (10 ml) with stirring in an ice bath. After solids were produced, the mixture was stored in a refrigerator overnight. The mixture were evaporated to dryness under reduced pressure and residue purified by column chromatography over silica gel (70–230 mesh), using ethyl acetate/hexane (V/V=1/4) as eluant to give a 40% yield of a colourless liquid. ^{1}H NMR ($CDCl_3$, TMS): δ(ppm) 1.38–1.39 (d, 3H, –CH*C**H**$_3$, J=6.4 Hz), 3.74–3.92 (m, 2H, –CH*C**H**$_2$OCH$_2$–), 3.91–4.02 (m, 2H, –CH$_2$OC**H**$_2$CF$_2$–), 5.31–5.34 (m, 1H, –COOC**H***CH$_3$), 7.29–7.31 (d, 2H, Ar**H**, J=8.5 Hz), 7.34–7.36 (d, 2H, Ar**H**, J=8.6 Hz), 8.10–8.12 (d, 2H, Ar**H**, J=8.5 Hz), 8.23–8.25 (d, 2H, Ar**H**, J=8.6 Hz).

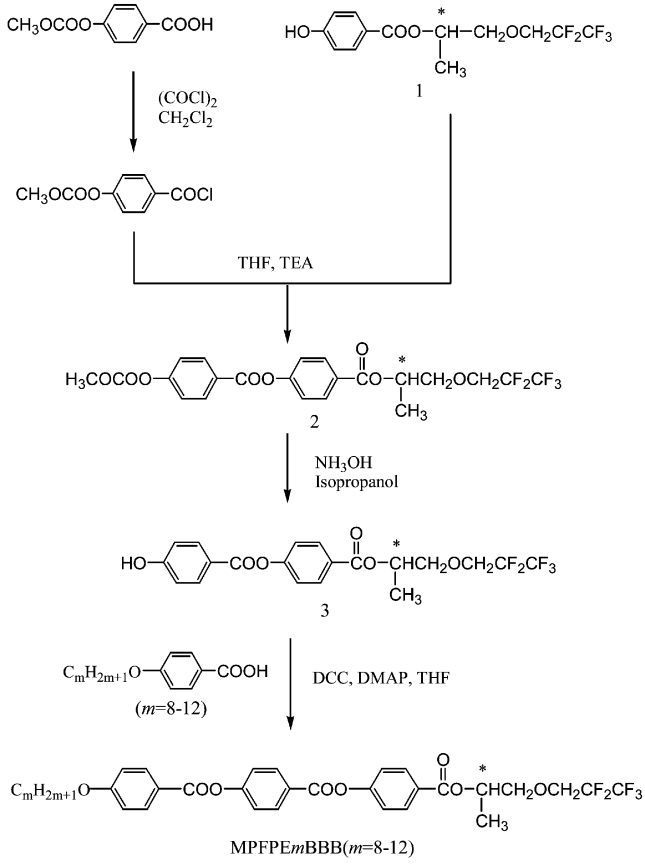

Scheme 1. Procedures for the synthesis of the chiral materials MPFPE*m*BBB(*m*=8–12).

2.2.4. (*R*)-1-Methyl-2-(2,2,3,3,3-pentafluoropropyloxy) ethyl 4-[4-hydroxybenzoyloxy]benzoate, 3. Material **2** (3.0 g, 6 mmol) was stirred in a mixture of isopropanol (90 ml) and ammonium hydroxide solution (28%, 30 ml) at room temperature for 50 min (TLC analysis revealed a complete reaction) and then poured into water (40 ml) with stirring. The product was extracted using

dichloromethane (3×50 ml). The combined organic extracts were washed with brine (3×50 ml), dried ($MgSO_4$), filtered and evaporated to give a colourless oil. The oil was purified by flash column chromatography over silica gel (70–230 mesh) using dichloromethane; the resulting oil was then dried in vacuum to give a 70% yield of material **3**. ^{1}H NMR ($CDCl_3$, TMS): δ(ppm) 1.45–1.47 (d, 3H, –CH*C**H**$_3$, J=7.0 Hz), 3.72–3.91 (m, 2H, –CH*C**H**$_2$OCH$_2$–), 3.98–4.05 (m, 2H, –CH$_2$OC**H**$_2$CF$_2$–), 5.26–5.27 (m, 1H, –COOC**H**CH$_3$), 5.40 (s, –O**H**), 6.82–6.84 (d, 2H, Ar**H**, J=8.5 Hz), 7.58–7.60 (d, 2H, Ar**H**, J=8.2 Hz), 7.62–7.64 (d, 2H, Ar**H**, J=8.0 Hz), 7.97–7.99 (d, 2H, Ar**H**, J=8.6 Hz).

2.2.5. (*R*)-4-[1-Methyl-2-(2,2,3,3,3-pentafluoropropyloxy)ethyl 4-{4-[4-(octyloxybenzoyloxy)benzoyloxy]}benzoate, MPFPE8BBB. A mixture of 4-octyloxybenzoic acid (0.9 g, 2.8 mmol), material **3** (1.2 g, 3.1 mmol), *N*,*N*′-dicyclohexylcarbodiimide (0.3 g, 2.8 mmol), 4-dimethylaminopyridine (0.05 g, 0.28 mmol) and dry THF (20 ml) was stirred at room temperature for 3 days. The precipitate was filtrated and the filtrate washed with 5% acetic acid solution (3×50 ml), 5% aqueous sodium hydrogen carbonate (3×50 ml) and water (3×50 ml), dried over anhydrous $MgSO_4$ and concentrated in vacuum. The residue was purified by column chromatography over silica gel (70–230 mesh) using dichloromethane as eluant. After recrystallization from absolute ethanol, a 50% yield of the target material was obtained. ^{1}H NMR ($CDCl_3$, TMS): δ(ppm) 0.88–0.90 (t, 3H, –CH$_2$C**H**$_3$, J=7.0 Hz), 1.28–1.50 (m, 13H, –OCH$_2$CH$_2$(C**H**$_2$)$_5$–, –OCH*C**H**$_3$–), 1.79–1.85 (m, 2H, –OCH$_2$C**H**$_2$–), 3.75–3.83 (m, 2H, –CH*C**H**$_2$O–), 3.91–4.07 (m, 4H, –CH$_2$OC**H**$_2$CF$_2$–, –C**H**$_2$OAr–), 5.31–5.34 (m, 1H, –COOC**H***CH$_3$–) 6.97–6.98 (d, 2H, Ar**H**, J=8.7 Hz), 7.31–7.33 (d, 2H, Ar**H**, J=7.0 Hz), 7.38–7.40 (d, 2H, Ar**H**, J=8.6 Hz), 8.11–8.13 (d, 2H, Ar**H**, J=8.6 Hz), 8.14–8.16 (d, 2H, Ar**H**, J=8.8 Hz), 8.28–8.29 (d, 2H, Ar**H**, J=8.4 Hz). IR (νmax/cm^{-1}): 2910, 2850 (C–H str.), 1733 (C=O str.), 1604, 1500 (aromatic str.), 1274 (C–F str.), 1203 (C–O str.), 840 (1, 4-disub. C–H o.o.p.b). Elemental analysis for $C_{35}H_{37}F_5O_8$: calculated, C 61.76, H 5.48; found, C 61.57, H 5.54%.

2.2.6. (*R*)-4-[1-Methyl-2-(2,2,3,3,3-pentafluoropropyloxy)ethyl 4-{4-[4-(nonyloxybenzoyloxy)benzoyloxy]}benzoate, MPFPE9BBB. This material was prepared in an analogous manner to MPFPE8BBB; yield 46%. ^{1}H NMR ($CDCl_3$, TMS): δ(ppm) 0.87–0.90 (t, 3H, –CH$_2$C**H**$_3$, J=7.2 Hz), 1.28–1.50 (m, 15H, –OCH$_2$CH$_2$(C**H**$_2$)$_6$–, –OCH*C**H**$_3$–), 1.77–1.84 (m, 2H, –OCH$_2$C**H**$_2$–), 3.76–3.83 (m, 2H, –CH*C**H**$_2$O–), 3.91–4.07 (m, 4H, –CH$_2$OC**H**$_2$CF$_2$–, –C**H**$_2$OAr–), 5.30–5.34 (m, 1H, –COOC**H***CH$_3$–) 6.97–6.98 (d, 2H, Ar**H**, J=8.7 Hz), 7.32–7.34 (d, 2H, Ar**H**, J=7.0 Hz), 7.38–7.40 (d, 2H, Ar**H**, J=8.6 Hz), 8.10–8.12 (d, 2H, Ar**H**, J=8.6 Hz), 8.14–8.16 (d, 2H, Ar**H**, J=8.8 Hz), 8.28–8.30 (d, 2H, Ar**H**, J=8.4 Hz). IR (νmax/cm^{-1}): 2920, 2845 (C–H str.), 1735 (C=O str.), 1604, 1500 (aromatic str.), 1270 (C–F str.), 1210 (C–O str.), 835 (1, 4-disub. C–H o.o.p.b). Elemental analysis for $C_{36}H_{39}F_5O_8$: calculated, C 62.24, H 5.66; found, C 61.97, H 5.80%.

2.2.7. (*R*)-4-[1-Methyl-2-(2,2,3,3,3-pentafluoropropyloxy)ethyl 4-{4-[4-(decyloxybenzoyloxy)benzoyloxy]}benzoate, MPFPE10BBB. This material was prepared in an analogous manner to MPFPE8BBB; yield 50%. ^{1}H NMR ($CDCl_3$, TMS): δ(ppm) 0.87–0.90 (t, 3H, –CH$_2$C**H**$_3$, J=7.5 Hz), 1.28–1.49 (m, 17H, –OCH$_2$CH$_2$(C**H**$_2$)$_7$–, –OCH*C**H**$_3$–), 1.80–1.85 (m, 2H, –OCH$_2$C**H**$_2$–), 3.75–3.83 (m, 2H, –CH*C**H**$_2$O–), 3.92–4.07 (m, 4H, –CH$_2$OC**H**$_2$CF$_2$–, –C**H**$_2$OAr–), 5.31–5.34 (m, 1H, –COOC**H***CH$_3$–) 6.98–6.99 (d, 2H, Ar**H**, J=8.8 Hz), 7.31–7.34 (d, 2H, Ar**H**, J=7.1 Hz), 7.37–7.39 (d, 2H, Ar**H**, J=8.7 Hz), 8.11–8.13 (d, 2H, Ar**H**, J=8.6 Hz), 8.14–8.16 (d, 2H, Ar**H**, J=8.8 Hz), 8.27–8.28 (d, 2H, Ar**H**, J=8.6 Hz). IR (νmax/cm^{-1}): 2919, 2852 (C–H str.), 1731 (C=O str.), 1606, 1509 (aromatic str.), 1272 (C–F str.), 1201 (C–O str.), 846 (1, 4-disub. C–H o.o.p.b). Elemental analysis for $C_{37}H_{41}F_5O_8$: calculated, C 62.71, H 5.83; found, C 62.57, H 5.8%.

2.2.8. (*R*)-4-[1-Methyl-2-(2,2,3,3,3-pentafluoropropyloxy)ethyl 4-{4-[4-(undecyloxybenzoyloxy)benzoyloxy]}benzoate, MPFPE11BBB. This material was prepared in an analogous manner to MPFPE8BBB; yield 42%. ^{1}H NMR ($CDCl_3$, TMS): δ(ppm) 0.87–0.90 (t, 3H, –CH$_2$C**H**$_3$, J=7.2 Hz), 1.28–1.50 (m, 19H, –OCH$_2$CH$_2$(C**H**$_2$)$_8$–, –OCH*C**H**$_3$–), 1.80–1.84 (m, 2H, –OCH$_2$C**H**$_2$–), 3.74–3.82 (m, 2H, –CH*C**H**$_2$O–), 3.93–4.07 (m, 4H, –CH$_2$OC**H**$_2$CF$_2$–, –C**H**$_2$OAr–), 5.31–5.34 (m, 1H, –COOC**H***CH$_3$–) 6.98–7.00 (d, 2H, Ar**H**, J=8.1 Hz), 7.32–7.34 (d, 2H, Ar**H**, J=7.8 Hz), 7.37–7.39 (d, 2H, Ar**H**, J=8.7 Hz), 8.11–8.13 (d, 2H, Ar**H**, J=8.6 Hz), 8.14–8.16 (d, 2H, Ar**H**, J=8.8 Hz), 8.27–8.29 (d, 2H, Ar**H**, J=8.4 Hz). IR (νmax/cm^{-1}): 2920, 2863 (C–H str.), 1731 (C=O str.), 1603, 1501 (aromatic str.), 1278 (C–F str.), 1213 (C–O str.), 833 (1, 4-disub. C–H o.o.p.b). Elemental analysis for $C_{38}H_{43}F_5O_8$: calculated, C 63.15, H 6.00; found, C 62.92, H 5.99%.

2.2.9. (*R*)-4-[1-Methyl-2-(2,2,3,3,3-pentafluoropropyloxy)ethyl 4-{4-[4-(dodecyloxybenzoyloxy)benzoyloxy]}benzoate, MPFPE12BBB. This material was prepared in an

Table 1. Mesophases, transition temperatures (°C) and associated enthalpy changa (kJ mol^{-1}, in brackets) for the chiral materials MPFPE*m*BBB(*m*=8–12).

m	I.		SmA*		SmC^*_α		SmC*		SmC^*_A		Cr	m.p.[b]
8	•	164.4 [8.6]	•		—		—	138.8 [0.3]	•	69.1 [47.0]	•	99.1 [46.0]
9	•	159.1 [8.1]	•	142.5 [c]	•	136.7 [0.5]	•	128.3 [d]	•	84.0 [49.6]	•	118.3 [57.3]
10	•	155.6 [8.4]	•	143.1 [0.4]	—		•	125.8 [d]	•	82.3 [51.9]	•	114.5 [54.8]
11	•	147.6 [6.4]	•	137.8 [0.5]	—		•		—	74.2 [38.7]	•	102.4 [41.5]
12	•	146.1 [9.1]	•	139.3 [1.0]	—		•		—	67.6 [31.4]	•	79.5 [31.4]

[a]Recorded by DSC thermograms at a cooling rate of 5°C min^{-1}. [b]Melting point taken from DSC thermograms at a heating rate of 5°C min^{-1}. [c]The temperature was confirmed by dielectric studies. [d]The enthalpy was too small to be determined by DSC.

analogous manner to MPFPE8BBB; yield 55%. ^{1}H NMR ($CDCl_3$, TMS): δ(ppm) 0.88–0.90 (t, 3H, –CH_2CH_3, J=7.0 Hz), 1.28–1.51 (m, 21H, –$OCH_2CH_2(CH_2)_9$–, –OCH*CH_3–), 1.81–1.84 (m, 2H, –OCH_2CH_2–), 3.74–3.82 (m, 2H, –CH*CH_2O–), 3.93–4.07 (m, 4H, –$CH_2OCH_2CF_2$–, –CH_2OAr–), 5.30–5.34 (m, 1H, –COOCH*CH_3–) 6.98–7.00 (d, 2H, ArH, J=8.0 Hz), 7.32–7.34 (d, 2H, ArH, J=8.0 Hz), 7.37–7.39 (d, 2H, ArH, J=8.7 Hz), 8.11–8.13 (d, 2H, ArH, J=8.6 Hz), 8.14–8.16 (d, 2H, ArH, J=8.8 Hz), 8.27–8.29 (d, 2H, ArH, J=8.4 Hz). IR (νmax/cm^{-1}): 2920, 2863 (C–H str.), 1731 (C=O str.), 1603, 1500 (aromatic str.), 1278 (C–F str.), 1210 (C–O str.), 840 (1, 4-disub. C–H o.o.p.b). Elemental analysis for $C_{39}H_{45}F_5O_8$: calculated, C 63.58, H 6.16; found, C 63.36, H 6.10%.

3. Results and discussion

3.1. *Mesomorphic properties*

The mesophases and their corresponding phase transition temperatures for MPFPE*m*BBB(*m*=8–12) were determined by texture observation using polarizing optical microscopy (POM) and differential scanning calorimetry (DSC), respectively. The SmA* phase was characterized by the formation of focal-conic texture, and the SmC* phase by the formation of striated focal-conic texture. The SmC^*_α phase is barely detectable by microscopy because its texture is similar to the SmC* phase, which may be due to the low tilt angle and a helical pitch which increases smoothly with decreasing temperature [11, 24, 25]; this anomaly was further detected by the measurement of dielectric constant. The SmC^*_A phase appeared as a striated focal-conic texture and was further investigated by the observation of switching current behaviour. The mesophases, transition temperatures, and enthalpies of transition for the chiral materials are listed in table 1. A plot of mesophase temperature versus the elongated alkyl chain length *m* for the materials is shown in figure 1. All the materials exhibited an enantiotropic SmA* phases whose temperature range and melting point decrease as the achiral chain lengthens. The SmC^*_A phase appears at the alkyl chain length *m*=8, 9 and 10. The SmC* phase appears at alkyl chain length greater than 9, its range becoming broader as the alkyl chain is lengthened. It was noted that one subphase, SmC^*_α, occurs at *m*=9.

Comparing the two semi-fluorinated materials, MPFPE10BBB and MPFPECP10BC (formula 2) [21],

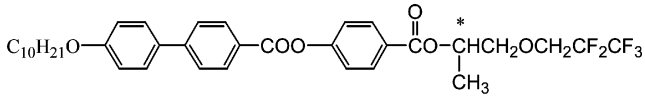

MPFPECP10BC

the former, which has a PhCOOPhCOOPhCOO core structure, shows the mesophases sequence I(155.6°C)-SmA*(143.1°C) SmC*(125.8°C)SmC^*_A(82.3°C)Cr; the latter, which has a PhPhCOOPhCOO core structure, shows the sequence I(158.8°C)SmA*(151.4°C)SmC*-(146.6°C)SmC^*_A(63.1°C)Cr. Both materials exhibit the same mesophses but the material with the PhPhCOOPhCOO core structure has a wider antiferroelectric SmC^*_A phase temperature range (83.5°C) than that with the PhCOOPhCOOPhCOO structure (43.8°C). It appears that the extension of the core structure suppress the stability of the SmC^*_A phase.

H. T. Nguyen *et al.* [8] reported that the tribenzoate material 10HHBBM7 (formula 3), with the (*R*)-1-

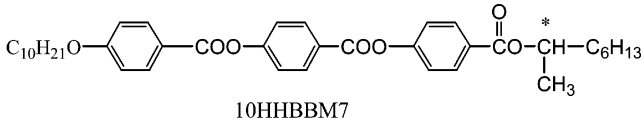

10HHBBM7

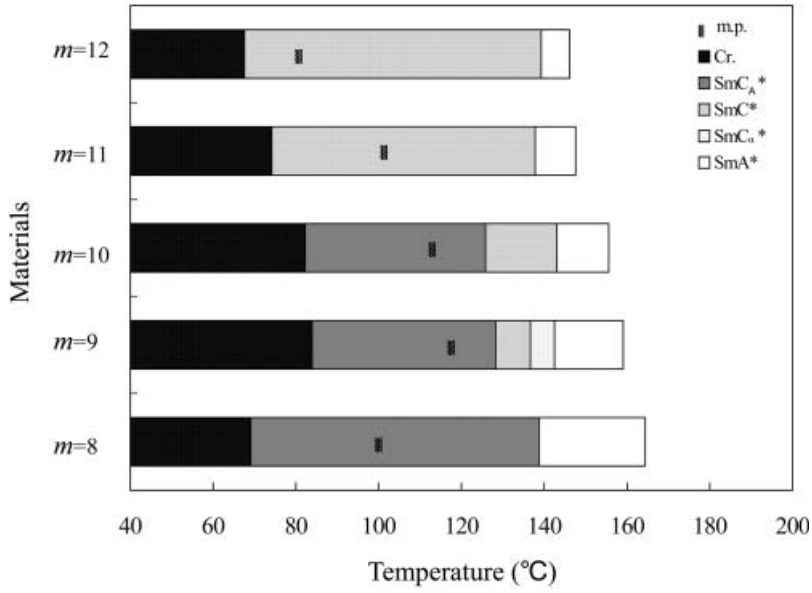

Figure 1. Chart of transition temperature as a function of terminal alkyl chain length for the chiral materials MPFPE*m*BBB(*m*=8–12) on cooling.

methylheptyl chiral group, displays a wide polymorphism, which includes the SmA*, SmC$^*_\alpha$, SmC*, SmC$^*_{FI2}$, SmC$^*_{FI1}$ and SmC$^*_A$ phases. Our results on the material MPFPECP10BB, with the semi-fluorinated alkyl chiral group, show that the tilted subphases SmC$^*_\alpha$, SmC$^*_{FI2}$ and SmC$^*_{FI1}$ phases are suppressed and the formation of the antiferroelectric phase enhanced.

3.2. *Physical properties*

The physical properties of the materials were measured in 5 µm homogeneous cells. Figure 2 shows the electrical switching response of MPFPE9BBB in a 5 µm thick homogeneous cell under a triangular wave voltage with field frequency of 1 Hz and an amplitude of 5 $V_{p\text{-}p}$. The switching current displays one current peak from 142°C to 128°C, similar to the behaviour reported for SmC$^*_\alpha$ and SmC* phases [26]. In the SmC$^*_A$ phase, however, two switching current peaks appeared, similar to the normal SmC$^*_A$ phase [26], supporting the existence of an antiferroelectric SmC$^*_A$ phase.

Figure 3 shows the temperature dependence of the dielectric constants ε for the material MPFPE9BBB measured at 100 Hz in 25 µm homogeneous cells. The ε in the SmA* phase is small. With decreasing temperature, ε increases slightly at the SmA*–SmC$^*_\alpha$ transition. In the

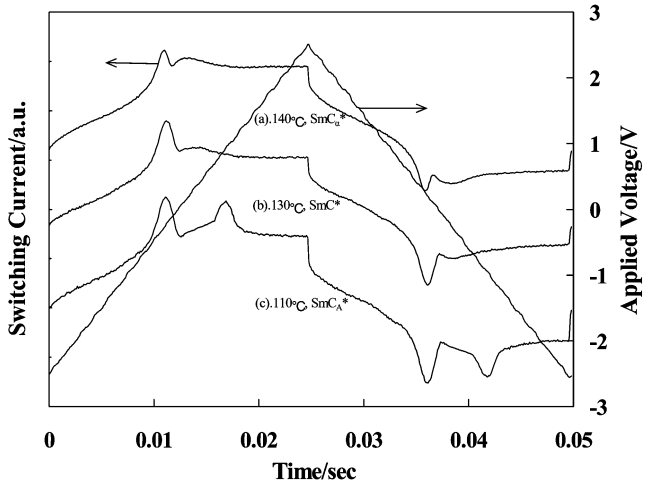

Figure 2. Switching current behaviour of MPFPECP9BB obtained at 1 Hz and several temperatures, on applying a triangular were in a 5 µm thick homogeneously alighned cell.

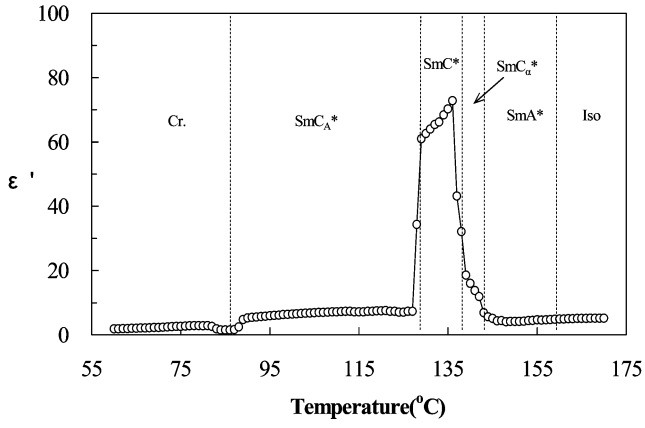

Figure 3. Temperature dependence of dielectric constant (ε') for MPFPE9BBB. The measurement was carried out at a cooling rate of 1°C min^{-1} and a frequency of 100 Hz.

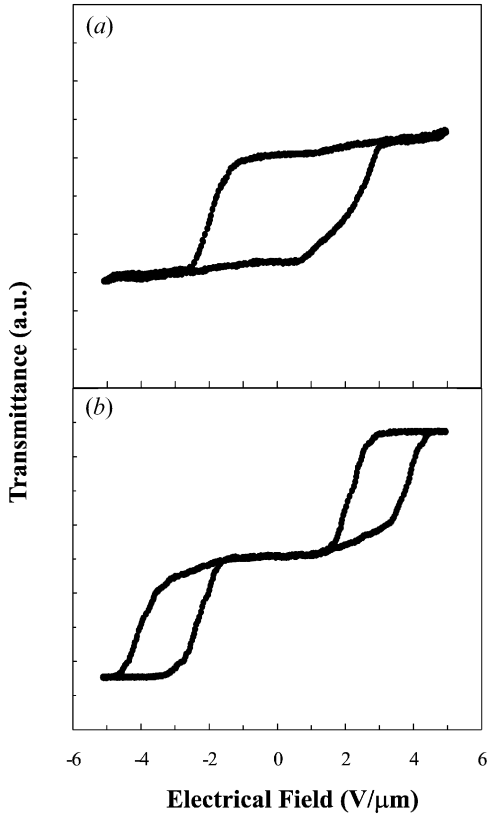

Figure 4. Electro-optical response of MPFPE9BBB (*a*) in the SmC* phase at 125°C, (*b*) in the SmC^*_A phase at 110°C, with 1 Hz frequency of applied triangular wave.

SmA* phase, close to the SmA*–SmC^*_α transition at about 142°C, the dielectric constant is enhanced slightly by the contribution of the tilt angle vibration (soft mode); in the SmC^*_α, the dielectric constant ε is enhanced due to the contributions of the vibration of the azimuthal molecular motions [26–30] and of the soft mode. Cooling to the SmC* phase at approximately 136°C, the dielectric constants increase rapidly due to the contribution of the Goldstone mode [30]. The dielectric constant falls to a very low value on further cooling from the SmC* phase to the occurrence of the SmC^*_A phase.

Electro-optical responses were obtained under crossed polarizers, with the axes of polarizer and analyser parallel and perpendicular, respectively, to the smectic layer normal, in 5 μm homogeneous aligned cells. Figure 4 illustrates the variation of transmittance with electric field on application of a triangular waveform field measured in the SmC* and SmC^*_A phase for MPFPE9BBB. It can be seen that at 125°C and 1 Hz frequency, the curves of transmittance versus applied field display an ideal single hysteresis in the SmC* phase, as shown in figure 4 (*a*). However, while cooling to 110°C, the curves display an ideal double hysteresis

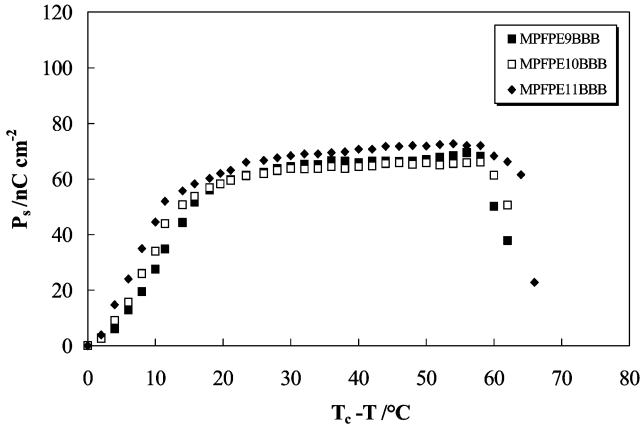

Figure 5. Spontaneous polarization plotted as a function of temperature for the materials MPFPE*m*BBB(*m*=9–11). T_c is the temperature of the SmA*–SmC* transition.

in the SmC^*_A phase, as shown in figure 4 (*b*). This corresponds to a tri-stable switching in the antiferroelectric state [1, 26], and is characteristic of a stable antiferroelectric phase.

The temperature dependence of the spontaneous polarization ($\mathbf{P}_s$) for MPFPE*m*BBB(*m*=9–11) was measured and is illustrated in figure 5. The measured maximum $\mathbf{P}_s$ values are in the range 66–72 nC cm^{-2}. Our previous study showed that the maximum $\mathbf{P}_s$ values for MPFPECP*m*BC (*m*=9–11) are in the range of 71–92 nC cm^{-2}, indicating that materials with PhPhCOOPhCOO as the core structure have a higher effective resulting molecular dipole than materials with PhCOOPhCOOPhCOO as the core structure.

Samples were sandwich-packed in 2 μm thick homogeneously aligned cells for the measurement of apparent tilt angle, using the usual 2θ optical method [31]. The temperature dependence of apparent title angle Θ of the materials is illustrated in figure 6. The tilt angles of the

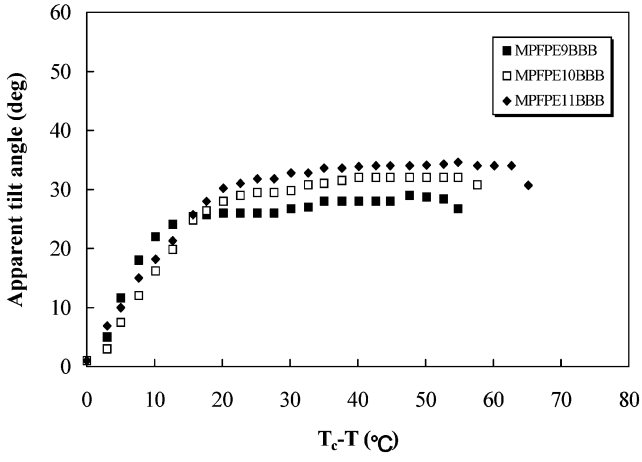

Figure 6. Temperature dependence of apparent tilt angle for the materials MPFPE*m*BBB(*m*=9–11).

materials are small at the SmA*–SmC* phase transition and increase as the temperature cools below the Curie point. Maximum apparent tilt angles in the range 29°–34° are obtained on further cooling. Our previous results showed that the maximum Θ values for MPFPECP*m*BC (*m*=9–11) are in the range 26°–33°, suggesting that the extendsion of the core structure has no significant effect.

4. Conclusion

We have demonstrated that the semi-fluorinated chiral materials MPFPE*m*BBB(*m*=8–12), derived from a tribenzoate core and a (*S*)-1-methyl-2-(2,2,3,3,3-pentafluoropropyloxy)ethyl chiral tail, exhibit an antiferroelectric SmC^*_A phase in the octyl to decyl members of the series. When compared with MPFPECP*m*BC, it can be seen that materials with PhPhCOOPhCOO as the molecular core structure are more favourable for the formation of the antiferroelectric SmC^*_A phase, and for higher $\mathbf{P}_s$ values, than those with PhCOOPhCOOPhCOO as the core structure. Moreover, when compared with the chiral materials *m*HHBBM7, it is found that the semi-fluorinated materials suppress the formation of tilted SmC^*_{FI2} and SmC^*_{FI1} subphases. These results imply that alkyl chain length, core structure and semi-fluorinated chiral tail play different roles in the formation of the antiferroelectric phase.

Acknowledgment

The authors are grateful for financial support of the National Science Council of the Republic of China (NSC 94-2216-E-036-008).

References

[1] A.D.L. Chandani, Y. Ouchi, H. Takezoe, A. Fukuda. *Jpn. J. appl. Phys.*, **27**, L729 (1988).
[2] A. Ikeda, Y. Takanishi, H. Takezoe, A. Fukuda. *Jpn. J. appl. Phys.*, **32**, L97 (1993).
[3] I. Nishiyama. *Adv. Mater.*, **6**, 12 (1994).
[4] S. Mery, D. Lötzsch, G. Heppke, R. Shashidhar. *Liq. Cryst.*, **23**, 5 (1997).
[5] W. Drzewiński, K. Czupryński, R. Dabrowski, M. Neubert. *Mol. Cryst. liq. Cryst.*, **328**, 401 (1999).
[6] Z. Raszwski, J. Kedziersji, J. Rutkowska, W. Piecek, P. Perpkowski, K. Czupryński, R. Dabrowski, W. Drzewiński, J. Zieliński, J. Zmija. *Mol. Cryst. liq. Cryst.*, **366**, 607 (2001).
[7] H.T. Nguyen, J.C. Rouillon, P. Cluzeau, G. Sigaud, C. Destrade, N. Isaert. *Liq. Cryst.*, **17**, 571 (1994).
[8] V. Faye, J.C. Rouillon, C. Destrade, H.T. Nguyen. *Liq. Cryst.*, **19**, 47 (1995).
[9] C.D. Cruz, J.C. Rouillon, J.P. Marcerou, N. Isaert, H.T. Nguyen. *Liq. Cryst.*, **28**, 125 (2001).
[10] C.D. Cruz, J.C. Rouillon, J.P. Marcerou, N. Isaert, H.T. Nguyen. *Liq. Cryst.*, **28**, 1185 (2001).
[11] S. Essid, M. Manai, A. Charbi, J.P. Marcerou, J.C. Rouillon, H.T. Nguyen. *Liq. Cryst.*, **31**, 1185 (2004).
[12] E. Dzik, J. Mieczkowski, E. Gorecka, D. Pociecha. *J. mater. Chem.*, **15**, 1255 (2005).
[13] V. Laux, N. Isaert, V. Faye, H.T. Nguyen. *Liq. Cryst.*, **27**, 81 (2000).
[14] S. Sarmento, P.S. Carvalho, M. Glogarova, M.R. Chaves, H.T. Nguyen, M.J. Ribeiro. *Liq. Cryst.*, **25**, 375 (1998).
[15] M.M. Jamshidi, H.T. Nguyen. *Ferroelectrics*, **310**, 73 (2004).
[16] S. Sarmento, P.S. Carvalho, M.R. Chaves, F. Pinto, H.T. Nguyen. *Liq. Cryst.*, **28**, 637 (2001).
[17] P.S. Carvalho, Y.I. Yuzyuk, A. Almeida, M.R. Chaves, F. Pinto, C.D. Cruz, H.T. Nguyen. *Liq. Cryst.*, **31**, 727 (2004).
[18] A. Cady, D.A. Olson, X.F. Han, H.T. Nguyen, C.C. Huang. *Phys. Rev. E*, **65**, 030701 (2001).
[19] S.T. Wang, Z.Q. Liu, B.K. McCoy, R. Pindak, W. Caliebe, H.T. Nguyen, C.C. Huang. *Phys. Rev. Lett.*, **96**, 097801 (2006).
[20] S.-L. Wu, C.-Y. Lin. *Liq. Cryst.*, **32**, 663 (2005).
[21] S.-L. Wu, C.-Y. Lin. *Liq. Cryst.*, **32**, 1053 (2005).
[22] K. Miyasato, S. Abe, H. Takezoe, A. Fukuda, E. Kuze. *Jpn. J. appl. Phys.*, **22**, L661 (1983).
[23] J. Lee, A.D. Chandani, K. Itoh, Y. Ouchi, H. Takezoe, A. Fukuda. *Jpn. J. appl. Phys.*, **29**, 1122 (1990).
[24] T. Isozaki, K. Hiraoka, Y. Takanishi, H. Takezoe, A. Fukuda, Y. Suzuki, I. Kawamura. *Liq. Cryst.*, **12**, 59 (1992).
[25] M. Skarabot, M. Cepic, B. Zebs, R. Bling, G. Heppke, A.V. Kityk, I. Masevic. *Phys. Rev. E*, **58**, 575 (1998).
[26] A. Fukuda, Y. Takanishi, T. Isozaki, K. Ishikawa, H. Takezoe. *J. mater. Chem.*, **4**, 997 (1994).
[27] K. Hiraoka, A. Taguchi, Y. Ouchi, H. Takezoe, A. Fukuda. *Jpn. J. appl. Phys.*, **29**, L103 (1990).
[28] K. Hiraoka, A.D.L. Chandani, E. Gorecka, Y. Ouchi, H. Takezoe, A. Fukuda. *Jpn. J. appl. Phys.*, **29**, L1473 (1990).
[29] Y. Takanishi, K. Hiraoka, V.K. Agrawal, H. Takezoe, A. Fukuda, M. Matsushita. *Jpn. J. appl. Phys.*, **30**, 2023 (1991).
[30] F. Gouda, K. Skarp, S.T. Lagerwall. *Ferroelectrics*, **113**, 165 (1991).
[31] K. Terashima, M. Ichihashi, M. Kikuchi, K. Furukawa, T. Inukal. *Mol. Cryst. liq. Cryst.*, **141**, 237 (1986).